



## Experimental

### *Materials*

The following materials were used as aluminium hydroxide specimens: hydrargillite-I and II (H-I, II), precipitated from sodium aluminate solution by seeding with hydrargillite-I and bayerite-II, respectively, at 30° [1]; bayerite-I and II (B-I, II), precipitated from sodium aluminate solution by interaction with a stream of carbon dioxide at 1 and 4 dm<sup>3</sup> min<sup>-1</sup> [1, 8], respectively; nordstrandite (N), prepared by aging amorphous aluminium hydroxide, precipitated from an aqueous 0.25 mol dm<sup>-3</sup> aluminium chloride solution by addition of 1 mol dm<sup>-3</sup> sodium hydroxide solution at pH 8, in an aqueous solution of ethylenediamine (~10%) for about a week at 40°.

These materials were examined by thermogravimetry and differential thermal analysis (TG and DTA), and the aluminium hydroxides and their thermal decomposition products by X-ray diffraction and infrared spectrophotometry, as described previously [17]. The decomposition products were prepared by heating the samples at the stated temperature for 2 hr after heating up to the temperature at a rate of 5 deg min<sup>-1</sup> under atmospheric pressure.

The TG and DTA were carried out on an automatic recording thermobalance and DTA apparatus (Agne Research Centre), using platinum-platinum/rhodium thermocouples and a Shinku-Riko Model TGD-1500RH-P differential thermobalance equipped with an infrared heater. For the measurement of differential thermal electromotive force,  $\alpha$ -alumina was used as a reference material. Specimens weighing 100–200 mg were heated at a rate of 5 deg min<sup>-1</sup> under atmospheric pressure. In the DTA at high temperature, however, the materials derived from the specimens preheated for 2 hr at the selected temperatures (700° for hydrargillite, 600° for bayerite and 600° for nordstrandite) weighed 300–450 mg.

## Results and discussion

TG and DTA curves for hydrargillite-I and II, bayerite-I and II and nordstrandite are illustrated in Figs 1–3. Table 1 gives representative X-ray diffraction results for the thermal decomposition products of the specimens. The infrared spectra of the aluminium hydroxides exhibit characteristic absorptions: for hydrargillite, the OH stretching band at 3700–3300 cm<sup>-1</sup>, the OH bending band at 1020 and 965 cm<sup>-1</sup> and the Al—OH vibration at 795–735 cm<sup>-1</sup>; for bayerite,  $\gamma$ -OH at 3700–3400 cm<sup>-1</sup>,  $\delta$ -OH at 1020 and 975 cm<sup>-1</sup> and Al—OH at

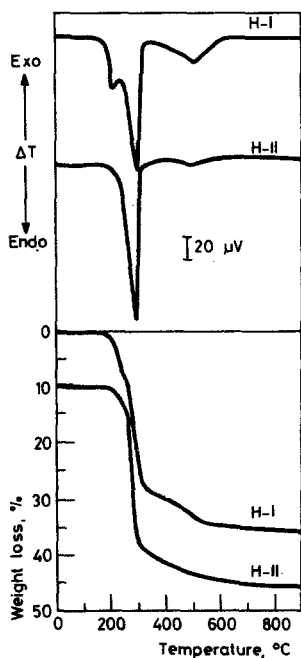


Fig. 1 TG and DTA curves of hydrargillite-I, II (H-I, II)

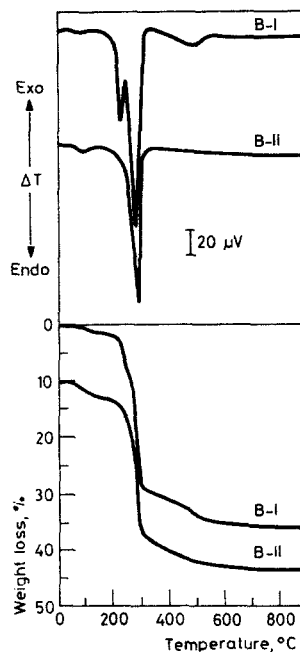


Fig. 2 TG and DTA curves of bayerite-I, II (B-I, II)

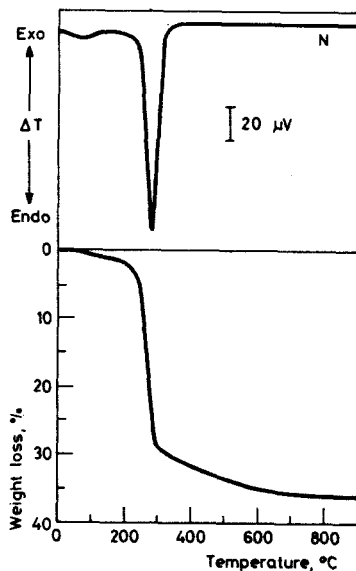


Fig. 3 TG and DTA curves of nordstrandite (N)

**Table 1** X-ray diffraction results of the products derived from crystalline aluminium hydroxides heated at various temperatures

Temp., °C	Phase detected				
	H-I	H-II	B-I	B-II	N
200	H + Bo	H	B + Bo	B	N
300	Bo + $\lambda$	$\lambda$	$\eta$ + Bo	$\eta$	$\eta$
400	Bo + $\lambda$	$\lambda$	$\eta$ + Bo	$\eta$	$\eta$
500	$\lambda$	$\lambda$	$\eta$	$\eta$	$\eta$
600	$\lambda$	$\lambda$	$\eta$	$\eta$	$\eta$
700	$\lambda$	$\lambda$	$\eta$	$\eta$	$\eta$
800	$\lambda$	$\lambda$	$\eta$ + $\theta$	$\eta$ + $\theta$	$\eta$ + $\theta$
900	$\lambda$ + $\kappa$	$\lambda$ + $\kappa$	$\theta$	$\eta$ + $\theta$	$\theta$ + $\eta$
1000	$\kappa$ + $\theta$	$\kappa$ + $\theta$	$\theta$	$\theta$	$\theta$
1100	$\theta$ + $\kappa$ + $\alpha$	$\kappa$ + $\theta$	$\theta$	$\theta$	$\theta$ + ( $\alpha$ ) <sup>a)</sup>
1200	$\alpha$ + $\theta$	$\kappa$ + $\theta$ + $\alpha$	$\alpha$ + $\theta$	$\theta$ + $\alpha$	$\theta$ + $\alpha$
1300	$\alpha$	$\alpha$ + $\theta$	$\alpha$	$\alpha$ + $\theta$	$\alpha$

<sup>a)</sup> Parenthesis indicates a small amount.

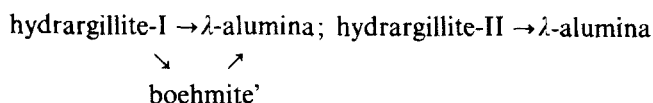
770–720  $\text{cm}^{-1}$ ; for nordstrandite,  $\gamma$ -OH at 3700–3300  $\text{cm}^{-1}$ ,  $\delta$ -OH at 1065, 980, 925 and 840  $\text{cm}^{-1}$  and Al—OH at 730  $\text{cm}^{-1}$  [17]. These absorption modes disappear completely during dehydration.

#### *Dehydration of crystalline aluminium hydroxides*

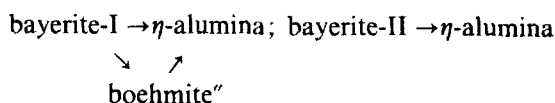
Hydrargillite and bayerite are classified as types I and II, respectively, according to the dehydration behaviour. Although the crystal structures of types I and II resemble each other somewhat, the particle sizes of the specimens H-I, II and B-I, II, determined with an Andreasen pipette, follow the sequence B-I, H-I, B-II, H-II. Microscopic examinations reveal that the particles of H-I and B-I are mostly single particles, while for H-II and B-II they are agglomerates of fine particles below 1  $\mu\text{m}$ .

The DTA curves in Fig. 1 show three endothermic reactions, at 210, 300 and 510°, for hydrargillite-I (coarse), and an endothermic one at 295° for hydrargillite-II (fine); these reactions occur at the points near the changes in shape of the TG curve. The weight loss at 1000° is 35.6% for types I and II, in agreement with the theoretical loss in weight of alumina trihydrate. The products formed at the endothermic peaks in the DTA curves indicate that hydrargillite-I dehydrates to a mixture of boehmite and hydrargillite at 210°, a mixture of boehmite and  $\lambda$ -alumina [1, 4] at 300°, and  $\lambda$ -alumina at 510°, while hydrargillite-II dehydrates directly to  $\lambda$ -alumina at 295°. As reported previously [1], it seems that the formation of boehmite during the dehydration depends on the effect of the water vapour pressure. When

the particles of the sample are coarse, the periphery of the particle approximates to the state formed with saturated water vapour, and boehmite is formed on the surface. This phenomenon does not occur with fine particles in the form of agglomerates. In this case, the structure of the boehmite resulting from the dehydration is identical with that of boehmite prepared by hydrothermal treatment, but the former boehmite is a poor crystallite. Thus, if we denote the boehmite formed during the dehydration of hydrargillite as boehmite', the dehydration of hydrargillite may be expressed by the following process:



Since bayerite is also of types I and II, the dehydration behaviour of bayerite resembles that of hydrargillite (Fig. 2). Bayerite-I (coarse) dehydrates to a mixture of boehmite and bayerite at 225°, a mixture of boehmite and  $\eta$ -alumina at 275°, and  $\eta$ -alumina at 505°, while bayerite-II (fine) dehydrates directly to  $\eta$ -alumina at 285°. At 1000°, the weight losses for types I and II are 35.9 and 33.6%, respectively, in agreement with the theoretical value for alumina trihydrate. Hence, it is expected that the dehydration process of bayerite is as follows:



where boehmite'' is designated in comparison with boehmite' for the dehydration process of hydrargillite.

The DTA curve for nordstrandite (Fig. 3) exhibits an endothermic reaction at 280°, corresponding to the change in the TG curve, and a loss in weight of 36.2% is observed at 1000°. This result resembles that for type II of bayerite and/or hydrargillite, and it is presumed that the dehydration behaviour of nordstrandite is more analogous to that of bayerite-II than to that of  $\eta$ -alumina at 300° (Table 1).

The thermal transformation of hydrargillite to  $\alpha$ -alumina has been studied by many researchers, and a number of sequences have been suggested for the stages through which the thermal transformation passes: boehmite,  $\chi$ -,  $\gamma$ -,  $\kappa$ -,  $\theta$ - and  $\alpha$ -aluminas [18]; boehmite,  $\kappa'$ -,  $\kappa$ - and  $\alpha$ -aluminas [19]; boehmite,  $\eta$  +  $\kappa'$ -,  $\kappa$ - and  $\alpha$ -aluminas [20]; boehmite,  $\gamma$ -,  $\delta$ -,  $\chi$ - and  $\alpha$ -aluminas [21]; boehmite,  $\varepsilon$ -,  $\kappa$ - and  $\alpha$ -aluminas [22]; boehmite,  $\chi$ -,  $\chi$ - and  $\alpha$ -aluminas [23]; and boehmite,  $\gamma$ -,  $\kappa$  +  $\theta$ - and  $\alpha$ -aluminas [24]. In contrast, Brown et al. [25] postulated a dual transformation in the thermal decomposition: hydrargillite dehydrates to boehmite and  $\chi$ -alumina at 200 and 300°, respectively; the boehmite formed is then transformed to  $\alpha$ -alumina at 1000° via  $\gamma$ -,  $\delta$ - and  $\theta$ -aluminas at 500, 800 and 900°, respectively, while  $\chi$ -alumina is

converted to  $\chi$ - and  $\alpha$ -aluminas at 800 and 1000°, respectively. Day et al. [26] reached a very similar conclusion relating to the origin of the two series of anhydrous products, but they assumed that the boehmite formed in the dehydration of hydrargillite is produced by a secondary reaction between the original dehydration product, the highly adsorbent  $\chi$ -alumina, and the water released during the reaction. Ginsberg et al. [27] also supported the sequence proposed by Brown et al. [25].

The thermal decomposition behaviour of hydrargillite is suggested to be dependent on many variables, and especially on the particle size of the samples of alumina hydrates. Thibon et al. [19] found that boehmite is not formed from hydrargillite with a very high specific surface. De Boer et al. [28] showed that hydrargillite dehydrates to  $\chi$ -alumina under normal conditions of water pressure, and to boehmite under hydrothermal conditions corresponding to the saturation pressure of water, and that hydrargillite with a larger grain size dehydrates to a mixture of boehmite and  $\chi$ -alumina, although hydrargillite gives  $\chi$ -alumina on dehydration. Tertian et al. [29] contended that fine hydrargillite dehydrates slowly to  $\alpha$ -alumina, via  $\chi$ - and  $\kappa$ -aluminas, while coarse hydrargillite dehydrates slowly to  $\alpha$ -alumina by two simultaneous routes, via  $\chi$ - and  $\kappa$ -aluminas, and via boehmite and  $\gamma$ -,  $\delta$ - and  $\theta$ -aluminas. Seafeld [30] concluded that relatively large crystals of hydrargillite follow the sequence boehmite,  $\gamma$ -,  $\theta$ - and  $\alpha$ -aluminas under hydrothermal conditions, and additionally the sequence  $\chi$ -,  $\kappa$ - and  $\alpha$ -aluminas during atmospheric heating. By using hydrargillite crystals  $< 1 \mu\text{m}$ , Brindly [31] found that several  $\kappa$ -type structures exist, and that, depending on the circumstances, one or other of these may be predominant, but not always the same structure. Goswami et al. [32] suggested that the thermal decomposition of hydrargillite proceeds in the sequence boehmite +  $\chi$ - and  $\kappa$ - +  $\gamma$ -aluminas for a well-crystalline sample, although the formation of boehmite is not observed for a poorly-crystalline one. In addition, Drobot et al. [33] suggested that hydrargillite dehydrates partly to boehmite and  $\gamma$ -alumina, and the boehmite is then again transformed to  $\gamma$ -alumina, which passes to  $\alpha$ -alumina via  $\theta$  +  $\kappa$ -aluminas. According to Lodding [34], however, when heated at constant rate, hydrargillite dehydroxylates partly to boehmite at  $\sim 250^\circ$  and partly to  $\kappa$ -alumina at  $250\text{--}330^\circ$ , and the boehmite is then transformed to  $\gamma$ -alumina at  $450\text{--}600^\circ$ ; the partial transformation of boehmite to  $\zeta$ -alumina is caused by the formation of an impervious layer; the onset and peak temperatures in the hydrargillite—boehmite step are controlled by the presence or absence of lattice substitutions and the heating rate, but are largely independent of the particle size and the surrounding atmosphere; the hydrargillite to  $\chi$ -alumina step is dependent on the particle size and lattice dislocations. Further, the formation of the boehmite phase and of microporous alumina during the thermal decomposition of hydrargillite at low pressure was examined by Rouquerol et al. [35].

The thermal transformation of bayerite to  $\alpha$ -alumina has been also studied by a number of researchers. Stumpf et al. [18] showed that the thermal transformation of bayerite proceeds through the stages boehmite,  $\eta$ -,  $\delta$ -,  $\theta$ - and  $\alpha$ -aluminas. Brown et al. [25] assumed that the  $\eta$ -alumina formed in the thermal decomposition of bayerite should be regarded as an extremely poorly-crystalline  $\gamma$ -alumina. Day et al. [26] suggested that, on calcination, bayerite yields  $\gamma$ -alumina, from which boehmite is formed only on hydration, and which on further calcination passes through  $\delta$ - and  $\theta$ -aluminas before finally yielding  $\alpha$ -alumina. Trokhimets et al. [36] reported the similar result that the formation of boehmite during dehydration stems from the dehydration of the amorphous alumina formed first. Alexanian [21] proposed the course of the thermal transformation of bayerite to  $\alpha$ -alumin via  $\gamma$ -,  $\delta$ - and  $\theta$ -aluminas. Tertian et al. [37] found that the calcination of bayerite produces successively  $\eta$ -,  $\theta$ - and  $\alpha$ -aluminas. Glemser et al. [22] considered that bayerite is thermally decomposed in the sequence boehmite-A,  $\eta$ -,  $\theta$ - and  $\alpha$ -aluminas. According to De Boer et al. [28], however, the dehydration of bayerite proceeds in a similar sequence to that for hydrargillite: bayerite with a larger grain size dehydrates to a mixture of boehmite and  $\gamma$ -alumina, while bayerite gives  $\gamma$ -alumina on dehydration.

As mentioned above, the author presumes that the dehydration behaviour of hydrargillite and of bayerite is influenced by the particle size of the samples used: hydrargillite-I (coarse) dehydrates to a mixture of boehmite and  $\lambda$ -alumina, while hydrargillite-II (fine) dehydrates to  $\lambda$ -alumina; bayerite-I (coarse) dehydrates to a mixture of boehmite and  $\eta$ -alumina, while bayerite-II (fine) dehydrates to  $\eta$ -alumina.

#### *Thermal transformation of anhydrous alumina to $\alpha$ -alumina*

The X-ray diffraction results (Table 1) on the products derived from crystalline aluminium trihydroxides heated at various temperatures indicate that the thermal transformation of anhydrous alumina to  $\alpha$ -alumina proceeds as follows: for hydrargillite,  $\lambda \rightarrow \kappa \rightarrow \theta \rightarrow \alpha$ ; for bayerite,  $\eta \rightarrow \theta \rightarrow \alpha$ ; for nordstrandite,  $\eta \rightarrow \theta \rightarrow \alpha$ . In contrast, the DTA curves of the materials derived from crystalline aluminium trihydroxides exhibit exothermic reactions due to the transformation of  $\theta$ -alumina to  $\alpha$ -alumina at 1290 and 1280° for hydrargillite-I and II, respectively, at 1230° for bayerite-I and II, and at 1260° for nordstrandite (Fig. 4). Accordingly, it is seen that the peak temperature for the transformation of  $\theta$ -alumina to  $\alpha$ -alumina for nordstrandite lies between those for hydrargillite and bayerite in the sequence H-I > H-II > N > B-I and II.

Hence, it is concluded that the aluminium hydroxides transform thermally to  $\alpha$ -alumina as follows:

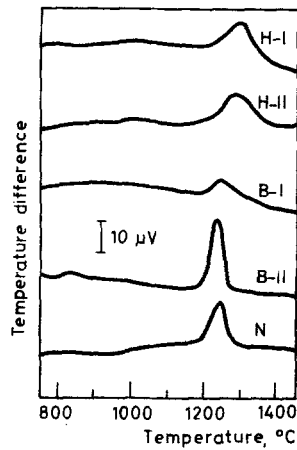
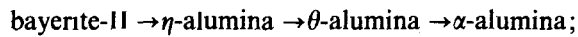
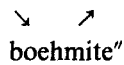
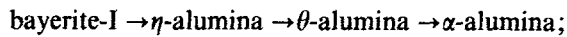
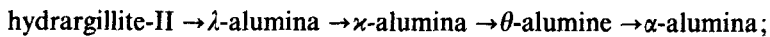
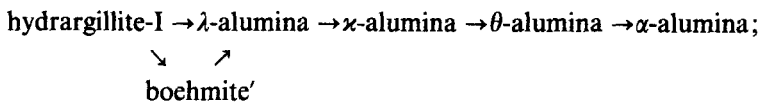
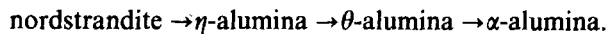


Fig. 4 DTA curves of the materials derived from hydrargillite, bayerite and nordstrandite preheated at 700, 600 and 600°, respectively, for 2 hrs (H-I, H-II; B-I, B-II; N)



and



\* \* \*

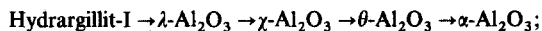
The author wishes to thank the Association for the Encouragement of Research in Light Metals (Keikinzoku Shogaku Kai) for a grant in connection with the present study.



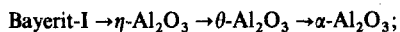
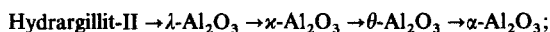
## References

- 1 T. Sato, *J. Appl. Chem.*, 9 (1959) 331 and therein cited literatures.
- 2 T. Sato, *J. Appl. Chem.*, 12 (1962) 9.
- 3 T. Sato, *J. Appl. Chem.*, 12 (1962) 553.
- 4 T. Sato, *J. Appl. Chem.*, 14 (1964) 303.
- 5 T. Sato, *Z. Anorg. Allgem. Chem.*, 391 (1972) 167.
- 6 T. Sato, F. Ozawa and S. Ikoma, *Proc. 6th Int. Conf. on Thermal Analysis*, Bayreuth, 1980, Vol. 2, p. 181 (1980), Birkhauser Verlag, Basel.
- 7 T. Sato, S. Ikoma and F. Ozawa, *Proc. 7th Int. Conf. on Thermal Analysis*, Kingston, 1983, Vol. 1, p. 578 (1983), John Wiley, Chichester.
- 8 T. Sato, T. Yamashita and F. Ozawa, *Z. Anorg. Allgem. Chem.*, 370 (1969) 202.
- 9 T. Sato, *Z. Anorg. Allgem. Chem.*, 391 (1972) 69.
- 10 T. Sato, *J. Appl. Chem. Biotechnol.*, 24 (1974) 187.
- 11 T. Sato, S. Ikoma and F. Ozawa, *J. Chem. Tech. Biotechnol.*, 30 (1980) 225.
- 12 T. Sato, *J. Chem. Tech. Biotechnol.*, 31 (1981) 670.
- 13 T. Sato, M. Suzuki and S. Ikoma, *J. Chem. Tech. Biotechnol.*, 31 (1981) 745.
- 14 T. Sato, *Proc. 9th Symposium on Industrial Crystallization*, The Hague, 1984, p. 385 (1984), Elsevier, Amsterdam.
- 15 T. Sato, *Proc. 9th Symposium on Industrial Crystallization*, The Hague, 1984, p. 391 (1984), Elsevier, Amsterdam.
- 16 T. Sato, F. Ozawa and S. Ikoma, *J. Appl. Chem. Biotechnol.*, 28 (1978) 811.
- 17 U. Hauschild, *Z. Anorg. Allgem. Chem.*, 324 (1965) 15.
- 18 H. C. Stumpf, A. S. Rusell, J. W. Newsome and C. M. Tucker, *Ind. Eng. Chem.*, 42 (1950) 1398.
- 19 H. Thibon, J. Charrier and R. Tertian, *Bull. Soc. Chim. Fr.*, (1951) 384.
- 20 M. Prettre, B. Imelik, L. Blanchin and M. Petitjean, *Angew. Chem.*, (1953) 65.
- 21 C. Alexanian, *Compt. Rend.*, 240 (1955) 1621.
- 22 O. Glemser and G. Rieck, *Angew. Chem.*, 67 (1955) 652.
- 23 K. Torker and H. Krischner, *Ber. Dtsch. Keram. Ges.*, 39 (1962) 131.
- 24 A. Velisar, A. Szabó and D. Tuclea, *Cercet. Metal., Inst. Cercet. Metal., Bucharest.*, 15 (1974) 467.
- 25 J. F. Brown, D. Clark and W. W. Elliot, *J. Chem. Soc.*, (1953) 84.
- 26 M. K. B. Day and V. J. Hell, *J. Phys. Chem.*, 57 (1953) 946.
- 27 H. Ginsberg, W. Hüttig and G. Strunk-Lichtenberg, *Z. Anorg. Chem.*, 293 (1957) 33.
- 28 J. H. de Boer, J. M. H. Fortuin and J. J. Steggerda, *Proc. Acad. Sci. Anst.*, 57B (1954) 170, 434.
- 29 R. Tertian and D. Papée, *J. Chim. Phys.*, 55 (1958) 341.
- 30 H. Seafeld, *Neues Jahrb. Mineral Abhandl.*, 95 (1960) 1.
- 31 G. W. Brindley and J. O. Choe, *Amer. Miner.*, 46 (1961) 771; G. W. Brindley, *ibid.*, 46 (1961) 1187.
- 32 K. N. Goswami and A. K. Gupta, *Trans. India Ceram. Soc.*, 36 (1977) 7.
- 33 N. M. Drobot, T. A. Mironenko and E. I. Khazanov, *Izv. Inst. Nefte-Uglekhim. Sin. Irkutsk Univ.*, 10 (1969) 50.
- 34 W. Lodding, *Proc. 2nd Int. Conf. on Thermal Analysis*, Worcester, Massachusetts, 1968, Vol. 2, p. 1239 (1969), Academic press, New York.
- 35 J. Rouquerol, F. Rouquerol and M. Ganteaume, *J. Catal.*, (1975) 36; (1979) 57.
- 36 A. I. Trokhimets, M. V. Waretskii and G. G. Kupchenko, *Vesti. Akad. Nauk B. SSR. Ser. Khim. Nauk.*, (1975) 119.
- 37 R. Tertian and D. Papée, *Compt. Rend.*, 241 (1955) 1575.

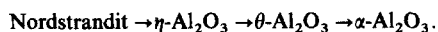
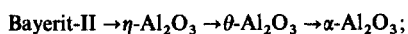
**Zusammenfassung** — Die thermische Zersetzung von kristallinen Aluminiumhydroxiden, wie Hydrargillit, Bayerit und Nordstrandit, wurde thermogravimetrisch, differentialthermoanalytisch, röntgendiffraktometrisch und IR-spektrophotometrisch untersucht. Es wurde festgestellt, daß diese Aluminiumhydroxide in der folgenden Reihenfolge zersetzt werden:



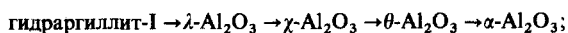
$\searrow \quad \nearrow$   
 Böhmit



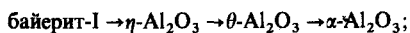
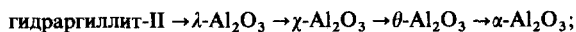
$\searrow \quad \nearrow$   
 Böhmit



**Резюме** — Методами термогравиметрии, дифференциального термического анализа, рентгеноструктурного анализа и ИК спектроскопии изучено термическое разложение таких кристаллических гидроокисей алюминия, как гидраргиллит, байерит и нордstrandит. Найдено, что эти соединения подвергаются термическому разложению в следующей последовательности:



$\searrow \quad \nearrow$   
 бозмит



$\searrow \quad \nearrow$   
 бозмит

